Asymmetric induction during electron transfer mediated photoreduction of carbonyl compounds: role of zeolites

J. Shailaja,[b] Lakshmi S. Kaanumalle,[a] Karthikeyan Sivasubramanian,[a] Arunkumar Natarajan,[a] Keith J. Ponchot,[b] Ajit Pradhan[b] and V. Ramamurthy*[a]

Received 1st December 2005, Accepted 7th February 2006
First published as an Advance Article on the web 14th March 2006
DOI: 10.1039/b517069a

Photochemistry of 17 aryl alkyl ketones included within cation exchanged zeolites has been examined. In solution five of the 17 ketones undergo intramolecular hydrogen abstraction reaction even in the presence of a chiral amine and the rest are photoreduced to the corresponding alcohol. Within zeolites all 17 ketones yielded in presence of a chiral amine, the corresponding alcohol as the major product. When a chiral amine was used as the coadsorbent within alkali ion exchanged zeolites, enantiomerically enriched alcohol was formed in all cases. The best chiral induction was obtained with phenyl cyclohexyl ketone (enantiomeric excess: 68%). ^{1}H–^{13}C Cross Polarization Magic Angle Spinning (CP-MAS) experiments, with a model ketone (perdeuterated acetophenone) and chiral amine (pseudoephedrine) included within MY zeolites, suggested that the cation brings the reactant and the chiral amine closer. The role of the cation in such a process is also revealed by the computation results. The results presented here highlight the importance of a supramolecular structure in forcing a closer interaction between a reactant and a chiral inductor that could be used to achieve asymmetric induction in photoproducts.

Introduction

During the last decade interest has been growing in the topic of asymmetric induction in photochemical reactions and a few remarkable methodologies have been developed.[1] In the early days of development, chiral solvents, circularly polarized light and chiral sensitizers were utilized to conduct enantioselective photoreactions and unfortunately they all yielded less than satisfactory results.[2,3] Recent efforts with chiral auxiliaries, chiral sensitizers and chiral templates have led to remarkable success.[4–6] Organized media have also been used to achieve asymmetric induction in photoreactions and of these, the crystalline state[7] and solid host–guest assemblies[8] have provided the most encouraging results. Our contribution to this topic has been to establish the utility of zeolites as media to achieve asymmetric induction.[9,10] In the absence of chiral zeolites, our approach has been to render the zeolite cages 'chiral' by absorption of an optically active molecule.

The strategy of employing chirally modified zeolite as a reaction medium requires inclusion of two different molecules: **C** (a chiral inductor) and **R** (a reactant), within the interior spaces of a zeolite. This strategy by its very nature does not allow quantitative chiral induction. When two different molecules **C** and **R** are included within a zeolite, the distribution is expected to follow the pattern shown in Fig. 1. The six possible modes of distribution of guest molecules are: type I (cages containing a single **C**), type II (two **C**'s), type III (single **R**), type IV (two **R**'s), type V (one **C** and one **R** molecule), and type VI (empty cages). The chiral induction obtained from the photoreaction of **R** is an average

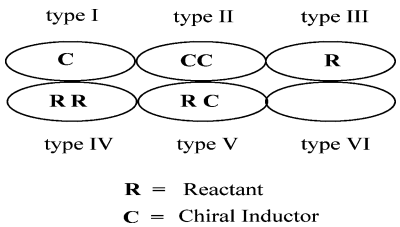

Fig. 1 Six possible modes of distribution of two different molecules, **C** and **R**, within zeolite supercages.

of the inductions that occur in cages of types III, IV (racemic products) and V (enantiomerically enriched product).

For the above approach to be successful (to avoid products from cages of types III and IV) every reactant molecule (**R**) has to be placed next to a chiral inductor molecule (**C**). Recognizing the current lack of knowledge concerning the distribution of guest molecules within a zeolite and the highly unlikely probability of placing every chiral inductor molecule next to a reactant molecule in the absence of any specific interaction between them, we have explored a strategy that would limit the photoreaction of interest to reactant molecules next to a chiral inductor. Such a condition eliminates the possibility of formation of the product of interest in the cages of types III and IV. The photoreaction we have investigated in this context is the well-known electron transfer initiated intermolecular hydrogen abstraction reaction of carbonyl compounds.[11] Under the conditions employed, one of the guest molecules (*e.g.*, ephedrine) assumes the dual role of a chiral inductor and an electron donor. We term such a strategy the 'chiral inductor as a reagent'. The goals of the current investigation are: (a) to explore the generality of the chiral inductor as a reagent strategy and (b) to establish that both the reactant ketone and chiral inductor molecules are present in a single supercage of a zeolite. For the former purpose we have investigated

[a]*Department of Chemistry, University of Miami, Coral Gables, Florida, 33124, USA. E-mail: murthy1@miami.edu; Fax: 305 284 4571; Tel: 305 284 1534*
[b]*Department of Chemistry, Tulane University, New Orleans, LA, 70118, USA*

the photoreduction of 17 aryl alkyl and diaryl ketones (**1a–1q**; Scheme 1) within chirally modified Y zeolites. To reach the second goal we have probed the model systems through solid state NMR and computational methods.

Results

To establish the versatility of zeolites to obtain high enantioselectivity, the chiral amine mediated photoreduction of 17 ketones (**1a–1q**) was investigated within alkali ion exchanged Y zeolite (Scheme 2). In solution, five of these ketones gave only products of intramolecular γ-hydrogen abstraction even in the presence of chiral amines. The remaining twelve ketones underwent photoreduction to the corresponding alcohol in the presence of chiral amines. No asymmetric induction was observed in solution. On the other hand, within zeolites all ketones gave the corresponding alcohol *via* an electron transfer process. Photoreduction was attempted with numerous chiral inductors whose structures are provided in Scheme 3.

A typical experimental procedure involved the addition of 250 mg of activated NaY zeolite to a solution of 7 mg (3.87×10^{-5} moles) of **1a–1q**, 26–30 mg of chiral inductor and 20 mL of hexanes. The mixture was allowed to stir under nitrogen for 2–3 h and then irradiated for 3 h. The conversions in most experiments were in the range of 20 to 35% as monitored by GC. The zeolite was filtered and the organic contents were extracted using acetonitrile. The chiral inductor was removed from the solution by column chromatography (silica gel/hexane–ethyl acetate) and the solution was concentrated and analysed using chiral GC/HPLC column. Both the reactant ketones and the product alcohols are known compounds and were synthesized by the literature methods (see experimental). Structures of the product alcohols were confirmed by comparing with authentic samples.

All 17 substrates, when irradiated within NaY zeolite in the presence of a suitable chiral amine, gave significant amounts of optically active alcohol (Scheme 2). The enantiomeric excesses (ee) obtained with ketones **1a–1q** included in NaY are listed in Table 1. For the sake of brevity we have provided results only in NaY. We have carried out experiments with several chiral amines in each case and the results reported correspond to the chiral amine that gave the best number. This clearly illustrates that there is no single chiral amine that works best for all ketones. The results (ee) obtained with various chiral inductors in the case of **1a** are summarized in Table 2. Data in Table 2 show that the extent of chiral induction depends on the structure of the chiral amine. Since detailed study was carried out only with ketone **1a**, the absolute configuration of the product alcohol in this case alone was identified by following the literature method.[12] In all other cases the first peak to elute from the chiral column is arbitrarily assigned as A and the second peak as B (Table 1). Once again

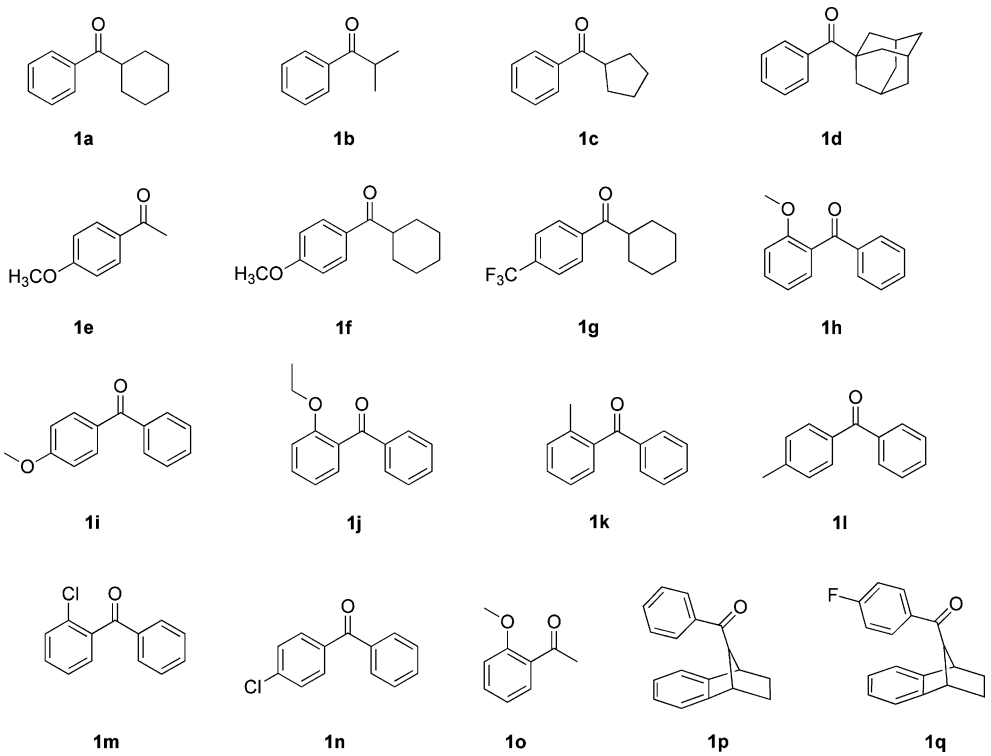

Scheme 1 List of aryl alkyl ketones investigated in this study.

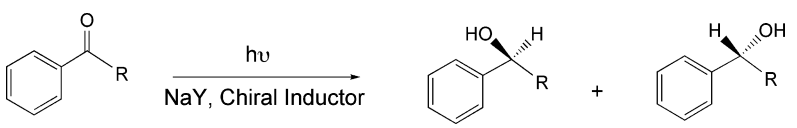

Scheme 2 Photoreduction of ketones within chirally modified NaY zeolite.

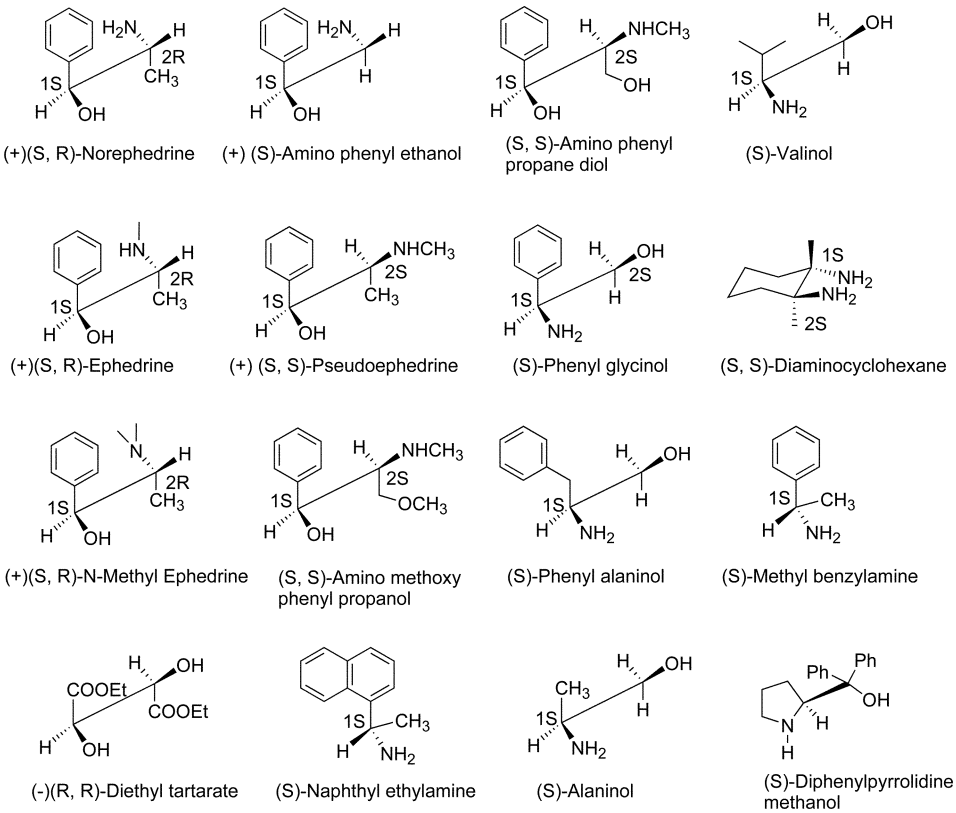

Scheme 3 Structures of chiral inductors explored in this study.

we wish to emphasize that no detailed studies on ketones **1b–1q** were conducted and a brief study on them helped us establish the generality of the zeolite based chiral induction strategy.

To probe the importance of alkali ions present in a zeolite in the chiral induction process several experiments were carried out with **1a**. The following observations are noteworthy: while the dry NaY containing optically pure norephedrine gave 68% ee, the same zeolite complex when it was intentionally made 'wet' by adsorption of water and irradiated gave <2% ee. Although the ee was influenced by the cation, the ratio of **2a** to **3a** remained the same under dry and wet conditions (for structures **2a** and **3a** see Scheme 5). We believe that hydrated Na^+ ions are unable to interact with the reacting ketone and the electron donor amine. If the cation present in a zeolite is important in aiding the necessary interaction between the ketone and the chiral inductor, the photoreduction and ee should depend on the nature and number of the cation. Y-Sil, a zeolite with morphology similar to Y zeolite but with very few cations gave negligible ee (<5%) with norephedrine as the chiral inductor. Similarly norephedrine when adsorbed onto MCM-41, a mesoporous zeolite, and silica gel containing no cation failed to induce enantioselectivity in the product alcohol. Examination of the photoreduction, with norephedrine as the chiral inductor within various alkali ion exchanged zeolites (LiY, NaY, KY, RbY and CsY), revealed that the nature of the cation is also important in the process of chiral induction. For the identical loading level of **1a** (one molecule per ten supercages) and norephedrine (one molecule per supercage), the ee within LiY, NaY, KY, RbY and CsY were 45%, 68%, 30%, 10% and zero respectively. From the above studies it is clear that the cation plays a crucial role during the chiral induction process and also that NaY is the best zeolite for the present purpose.

To establish the role of a cation in bringing the reactant ketone and the chiral amine closer we have carried out NMR polarization experiments of solid zeolite samples. Solid state NMR experiments such as intermolecular ^1H–^{13}C Cross Polarization Magic Angle Spinning (CP-MAS) can provide insight into the existence of interactions between adsorbed molecules within a zeolite and can also provide evidence regarding the relative proximity of the two molecules.[13–16] In a CP-MAS experiment, the CP part of the experiment involves selective ^1H magnetization followed by dipolar transfer to the less abundant ^{13}C nuclei under Hartman–Hahn matching conditions. Our study was prompted by the work of Garcia-Garibay and co-workers on benzophenone and cyclohexane in NaY.[16] By comparison of the ^{13}C signal intensities of benzophenone, due to ^1H–^{13}C Cross Polarization Magic Angle Spinning (CP-MAS) measured with deuterated and non-deuterated benzophenone samples, Garcia-Garibay and co-workers established that the intermolecular C–D–H–R distances between carbon atoms of deuterated benzophenone and hydrogens of cyclohexanes have an average value of *ca.* 2.2 Å within NaY. This suggested that CP-MAS experiments could be useful in establishing the presence of an interaction between the cation, the ketone and the chiral inductor.

The CP-MAS experiments were carried out with perdeuterated acetophenone as the ketone and pseudoephedrine as the chiral amine. The choice of acetophenone as the model compound was dictated by the ready availability of deuterated acetophenones such as $C_6H_5COCD_3$, $C_6D_5COCH_3$ and $C_6D_5COCD_3$. The observation

Table 1 Enantiomeric excess in the alcohol products of ketones **1a–1q** included in NaY zeolite in presence of a chiral inductor[a,b]

Substrate	Zeolite	Chiral inductor	%Enantiomeric excess[c,d]
1a	NaY	(+)-Norephedrine	68*R*
1b	NaY	(−)-Norephedrine	67*S*
1b	NaY	(+)-Norephedrine	50
1c	NaY	(+)-Pseudoephedrine	30
1d	NaY	(+)-Pseudoephedrine	25
1e	NaY	(+)-Ephedrine	47A
1e	NaY	(−)-Ephedrine	53B
1f	NaY	(+)-Pseudoephedrine	30
1g	NaY	(+)-Ephedrine	35
1h	NaY	(1*R*,2*R*)-(1,2-Diaminocyclohexane)	42B
1h	NaY	(1*S*,2*S*)-(1,2-Diaminocyclohexane)	44A
1i	NaY	(−)-Ephedrine	40B
1i	NaY	(+)-Ephedrine	42A
1j	NaY	(+)-Pseudoephedrine	43A
1j	NaY	(−)-Pseudoephedrine	43B
1k	NaY	(−)-Pseudoephedrine	36B
1k	NaY	(+)-Ephedrine	24A
1k	NaY	(−)-Ephedrine	23B
1k	NaY	(+)-Pseudoephedrine	28A
1l	NaY	(−)-Pseudoephedrine	22A
1l	NaY	(+)-Pseudoephedrine	22B
1m	NaY	(+)-Pseudoephedrine	24A
1m	NaY	(−)-Ephedrine	34B
1n	NaY	(+)-Pseudoephedrine	24A
1n	NaY	(−)-Pseudoephedrine	23B
1o	NaY	(+)-Pseudoephedrine	30A
1o	NaY	(−)-Pseudoephedrine	27B
1p	NaY	(−)-Ephedrine	64B
1p	NaY	(+)-Ephedrine	65A
1q	NaY	(−)-Ephedrine	57B
1q	NaY	(+)-Ephedrine	58A

[a] The numbers reported are the average of at least three independent runs. [b] The loading level was maintained at one ketone per 10 supercages and one chiral amine per cage. [c] In the case of ketone **1a**, the absolute configuration of the product alcohol has been identified. *R* and *S* refer to the isomer being enhanced. [d] In ketones **1b–1q** the absolute configuration of the product alcohol was not identified. The first peak to elute from the GC or HPLC column was noted as A and the second as B.

Table 2 Enantiomeric excess of alcohol product of ketone **1a** with various chirally modified NaY zeolites[a,b]

Medium	Chiral inductor	%Enantiomeric excess[c]
NaY	(+)(*S*,*R*)-Norephedrine	68*R*
NaY	(−)(*R*,*S*)-Norephedrine	67*S*
NaY	(+)(*S*)-Aminophenylethanol	26*R*
NaY	(*S*,*S*)-Aminophenylpropanediol	54*S*
NaY	(*S*)-Valinol	9*S*
NaY	(*R*)-Valinol	10*R*
NaY	(+)(*S*,*R*)-Ephedrine	16*R*
NaY	(−)(*R*,*S*)-Ephedrine	11*S*
NaY	(+)(*S*,*S*)-Pseudoephedrine	37*R*
NaY	(−)(*R*,*R*)-Pseudoephedrine	35*S*
NaY	(*S*)-Phenylglycinol	11*R*
NaY	(*S*,*S*)-Diaminocyclohexane	26*S*
NaY	(+)(*S*,*R*)-*N*-methylephedrine	27*R*
NaY	(−)(*R*,*S*)-*N*-methylephedrine	23*S*
NaY	(*S*,*S*)-Aminomethoxyphenylpropanol	30*S*
NaY	(*S*)-Phenylalaninol	13*R*
NaY	(*S*)-Methylbenzylamine	8*S*
NaY	(*S*)-Alaninol	2*S*
NaY	(*S*)-Diphenylpyrrolidine methanol	25*R*

[a] The numbers reported are the average of at least three independent runs. [b] The loading level was maintained at one ketone per 10 supercages and one chiral amine per cage. [c] In the case of ketone **1a**, the absolute configuration of the product alcohol has been identified. *R* and *S* refer to the isomer being enhanced.

of ^{13}C signals from perdeuterated acetophenone relies on the polarized ^{1}H source and cannot be observed unless we have a hydrogen source that is relatively rigid and is in closer proximity to the perdeuterated acetophenone molecule. The absence of ^{13}C signals in the ^{1}H–^{13}C CP-MAS spectra of perdeuterated acetophenone adsorbed within NaY indicates that there is no source of hydrogen present inside the zeolite from which the polarization transfer could take place. But when ^{1}H–^{13}C CP-MAS spectra of perdeuterated acetophenone and (−)-pseudoephedrine adsorbed within NaY were recorded, along with the signals of the chiral inductor, a new ^{13}C signal at δ 25 ppm was observed. Based on the fact that the ^{13}C signal of CH_3 in acetophenone comes at δ 25 ppm, we assign the new ^{13}C signal at δ 25 ppm to be that of CD_3, perdeuterated acetophenone. The maximum distance up to which intermolecular polarization transfer can take place is 10 Å and since the diameter of the supercage is 13 Å, it is quite possible that both the chiral inductor and perdeuterated acetophenone are present in the same or adjacent supercages of NaY.

Support for the above interaction between the ketone and the amine also comes from the contact time variation study. In this study we assume that the polarization transfer occurs through interaction between the ^{1}H of (−)-pseudoephedrine and the ^{13}C of perdeuterated acetophenone. Cations are assumed not to play a role in this process. In a ^{1}H–^{13}C CP-MAS experiment, the ^{13}C

signals grow during ^{1}H–^{13}C contact times and then decay by virtue of their spin lattice relaxation. If the polarization transfer is taking place between two molecules (intermolecular), the intensity of the new ^{13}C signal observed should increase with the increase in contact time. As shown in Fig. 2, when ^{1}H–^{13}C CP-MAS spectra of (−)-pseudoephedrine and perdeuterated acetophenone adsorbed within NaY were recorded with varying contact times (2500 μs to 50 μs), the intensity of the ^{13}C signal due to CD_3 at δ 25 was at a maximum when the contact time was 2500 μs and it decreased with the decrease in contact time. In order to provide further support for the above proposition of intermolecular polarization transfer, a contact time variation study of (−)-pseudoephedrine and acetophenone ($C_6H_5COCH_3$) adsorbed within NaY was performed. Unlike the perdeuterated acetophenone case, here the proton source required for polarization transfer is present within the acetophenone molecule itself and hence one would expect no significant change in the relative intensity of the signal with varying contact times used in this study. The contact time variation did not affect the relative intensity of the ^{13}C signal due to the CH_3 of acetophenone at δ 25 in the contact time range of 50–2500 μs.

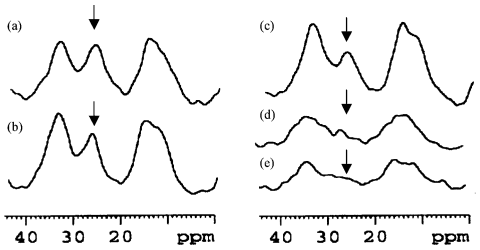

Fig. 2 Contact time dependent ^{1}H–^{13}C CP-MAS spectra for (−)-pseudoephedrine and perdeuterated acetophenone adsorbed within NaY zeolite. Only a narrow region corresponding to the ^{13}C signal due to CD_3 is shown. The arrow points to the ^{13}C signal due to CD_3. Note the intensity change with contact time. The other signals correspond to (−)-pseudoephedrine. (a) 2500 μs, (b) 1500 μs, (c) 500 μs, (d) 300 μs and (e) 50 μs.

The importance of the charge density of the cation in bringing the ketone and chiral amine closer is evident when ^{1}H–^{13}C CP-MAS spectra of perdeuterated acetophenone and (−)-pseudoephedrine adsorbed within Li^+, Na^+ and K^+ exchanged Y zeolites for the same loading level of ketone and chiral inductor were recorded. It can be inferred from Fig. 3 that, on going from Li^+ to K^+, the intensity of the ^{13}C signal due to CD_3 (δ = 25 ppm) changed with the relative intensity being large in LiY and smaller in KY. Because of the poor baseline, the intensities of the signals are not reliable and therefore no quantitative comparison between the cations could be made. Alternative experiments of varying the contact time to achieve the same intensity were not conducted. However the importance of zeolite framework and cations is revealed when ^{1}H–^{13}C CP-MAS spectra of (−)-pseudoephedrine and perdeuterated acetophenone adsorbed on silica gel were recorded. From the spectra in Fig. 3 it is clear that the intensity of the new signal was least when silica gel was used as a medium, suggesting that silica gel that lacks cations is not able to interact strongly with the adsorbed organic molecules and thus bring them closer for intermolecular polarization transfer to occur.

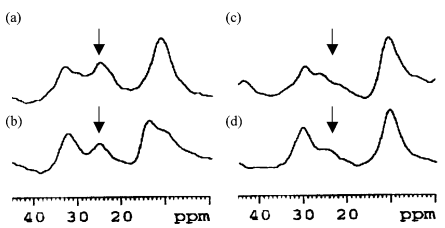

Fig. 3 ^{1}H–^{13}C CP-MAS spectra for (−)-pseudoephedrine and perdeuterated acetophenone adsorbed within alkali ion exchanged Y zeolites and onto silica gel. Only a narrow region corresponding to the ^{13}C signal due to CD_3 is shown. The arrow points to the ^{13}C signal due to CD_3. Note the intensity change with the nature of the alkali ion present in a zeolite. Other signals correspond to (−)-pseudoephedrine. (a) LiY, (b) NaY, (c) KY and (d) silica gel.

Results of ^{1}H–^{13}C CP-MAS experiments confirm that there are cages of type V (Fig. 1) within NaY zeolites. We believe that photoreduction occurs in such cages. To provide further support to our assumption that the cation plays an important role in the chiral induction process we decided to probe, through computations, the possibility of a cation forcing an interaction between the reactant ketone **1a** and norephedrine. Computations were carried out with the Gaussian 98 suite of programs at the RB3LYP level with the 6–31G(*) basis set.[17] The goal of the computations is simple: can an alkali ion force an interaction between a reactive ketone and a chiral amine? We recognize that the computationally generated structures that refer to the gas phase may be of limited value in the development of a mechanistic model where the cations are embedded within the walls of a zeolite. Although the computations relate to free cations, we felt that the trends observed in the gas phase would be useful in gaining an insight into the origin of chiral induction within a zeolite.

Computations with (+)-norephedrine, phenyl cyclohexyl ketone (**1a**) and Li^+ were performed in three stages. In stage 1, the most computationally favored conformations of the chiral amine, (+)-norephedrine, were determined. In stage 2, the Li^+ ion was allowed to interact with the conformers of (+)-norephedrine to determine the computationally favored structures for the Li^+–chiral amine complex. In the final stage, the ketone was allowed to interact with the Li^+–chiral amine complex.

Chiral inductor molecule (+)-norephedrine on geometry optimization at RB3LYP/6-31G* level, resulted in three conformers close in energy (difference in energies <1 kcal mol^{-1}). Energies and optimized structures of the conformers are shown in Fig. 4. The three conformers represent the three Newman projections that would be obtained for norephedrine. In two of these, as expected, there is hydrogen bonding between the amino and hydroxyl groups. The structures and energies reported here are similar to the ones recently computed at the MP2/6-311 + G** level by Simons and co-workers.[18]

Each conformer was independently allowed to interact with Li^+ ion, and re-optimized. During the calculation, Li^+ ion was free to move to find the most stable position. Seven structures were obtained, inclusive of bidentate and monodentate interactions of Li^+ with (+)-norephedrine (Fig. 5). In the bidentate modes shown in Figs. 5a–c, Li^+ interacted with amino nitrogen and hydroxyl oxygen in **a**, amino nitrogen and phenyl in **b**, hydroxyl oxygen and phenyl in **c** and in the monodentate modes shown in Figs. 5d–g it interacted with amino nitrogen in **d**, hydroxyl oxygen in **e**, phenyl from face-1 in **f** and with phenyl from face-2 in **g**.

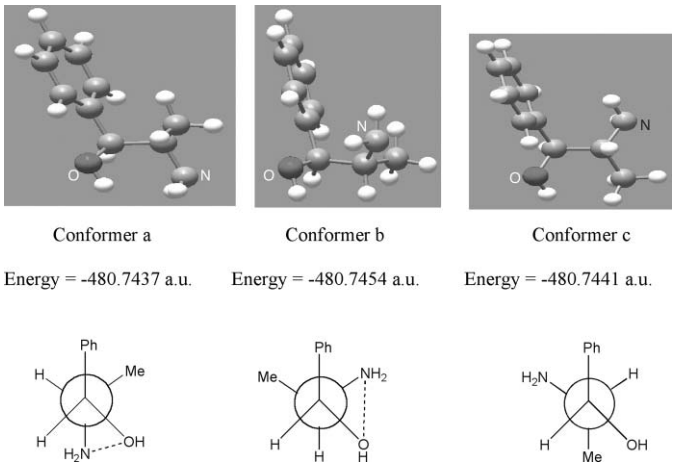

Fig. 4 The three conformers of (+)(1*S*,2*R*)-norephedrine chiral inductor optimized at the RB3LYP level with the 6-31G* basis set in Gaussian 98.

Assuming the least stable structure as zero, the relative energies of various structures are listed in Fig. 5. Perusal of Fig. 5 reveals that structures in which cation is bound to two functional groups (**a–c** in Fig. 5) are more stable than those possessing a single interaction (**d–g** in Fig. 5). According to computation, the cation interacting with amino nitrogen and alcohol oxygen is the most stable (structure **a** in Fig. 5).

Structure **a** in Fig. 5 was re-optimized at the RB3LYP/6-31G* level in the presence of cyclohexyl phenyl ketone. During the calculation, the alkali ion was free to move to find the most stable position. Calculations were repeated by placing the alkali ion at various locations. Independent of the starting location of the cation, structure **h** shown in Fig. 6 was obtained for the supramolecular complex of Li^+, cyclohexyl phenyl ketone and norephedrine. It is important to note in structure **h** that a newer interaction between Li^+ cation and the carbonyl of the cyclohexyl

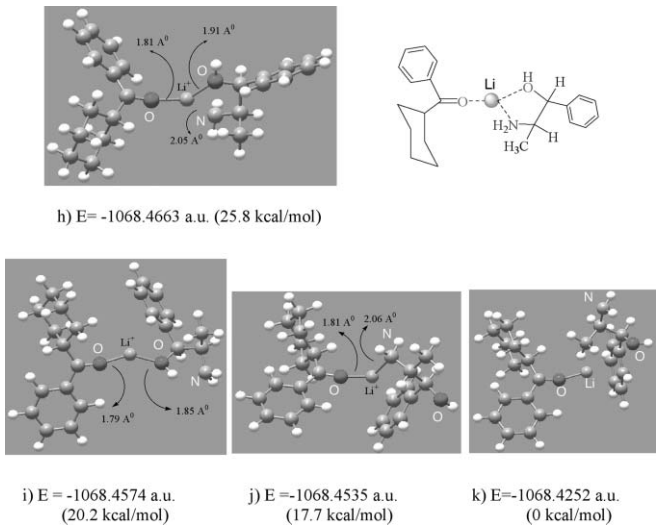

Fig. 6 Interaction between the ketone, lithium cation and (+)-norephedrine chiral inductor in the gaseous state as obtained by computations. The relative energy differences in kcal mol^{-1} between the given complex **k** and the conformers **h–j** are shown in parentheses.

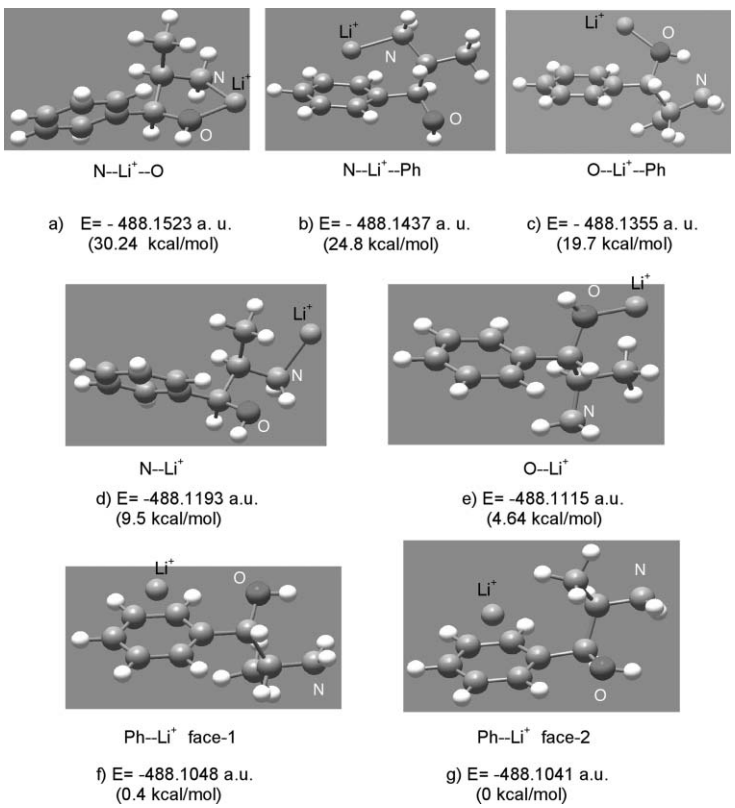

Fig. 5 Various modes of lithium cation binding to (+)-norephedrine chiral inductor (Gaussian 98/RB3LYP/6-31G*). The relative energy differences in kcal mol^{-1} between the given conformer **g** and the most stable conformers **a–f** are shown in parentheses.

phenyl ketone has developed. To identify other possible structures for the ternary complex, structures **b–g** in Fig. 5 were independently optimized in the presence of cyclohexyl phenyl ketone at the RB3LYP/6-31G* level. Three supramolecular structures (**i–k** in Fig. 6) were obtained. Vibrational frequencies with no Raman intensities were computed for all four structures and were found to be positive. Positive frequencies suggest that all three cation bound structures are true minima. We do not know which one of the four structures is present within a zeolite. Independent of this limitation the computational results unequivocally suggest that an alkali ion can bring a reactive ketone and an electron transfer agent, chiral amine, closer. Existence of closer interaction between alkali ion, reactive ketone and chiral amine is consistent with the results of CP-MAS experiments and photochemical product studies.

Discussion

From the results presented above it is clear that the phenomenon of asymmetric induction during electron transfer mediated photoreduction within alkali ion exchanged zeolites is general. Cations present within a zeolite play an important role in this process. The results of solid-state NMR experiments and computational studies suggest that alkali ions help to bring the reactant ketone and the chiral amine closer.

Perusal of Table 1 reveals that ketones **1a**, **1b**, **1e**, **1i**, **1p** and **1q** give moderate enantioselectivity (e.e) within NaY: **1a**, (+)-norephedrine (68%); **1b**, (+)-norephedrine (50%); **1e**, (−)-ephedrine (53%); **1i**, (+)-ephedrine (42%); **1p**, (−)-ephedrine (64%) and **1q**, (−)-ephedrine (57%). We recognize that the ee obtained is certainly not in the range to be synthetically useful. However, we wish to emphasize that our studies are directed towards understanding supramolecular interactions and in this context the results reported here are significant. One of the earliest reports of the use of amines as chiral reagents is by Seebach and coworkers in the solution phase photopinacolization of aromatic ketones.[19] A mixture of 1 : 5 chiral amine to pentane as solvent at −72 °C gave about 23.5% ee in the DL-pinacol formed from acetophenone. It is important to note that in our studies no pinacol was obtained and in the majority of the cases the only product is the corresponding alcohol and the ee obtained within zeolites is in the range between 22–68%. When the irradiation was carried out in solution in all cases only racemic products were obtained.

The general mechanism of amine-mediated photoreduction of carbonyl compounds is shown in Scheme 4.[11] This process involves three steps: first, an electron transfer from the amine to the excited carbonyl chromophore, second, proton transfer from the radical cation to the radical anion and third, the reaction of the radical intermediates, yielding either a pinacol or the corresponding alcohol. One of the important aspects of this reduction is that it is independent of the nature of the lowest excited state (nπ* or ππ*) of the reacting carbonyl compound. The mechanism shown in Scheme 4 works best for primary and secondary amines, but tertiary amines also initiate photoreduction through an electron transfer pathway. We believe that photoreduction of all ketones examined in this study proceeds by the electron transfer pathway shown in Scheme 4. Although we carried out preliminary studies on 17 ketones, in depth investigation was pursued only on ketone **1a**. As emphasized earlier, the study on the other sixteen ketones helped us establish the generality of the zeolite based 'chiral inductor as a reagent' strategy. However, we are unable to establish any structure–asymmetric induction relationship with the ketones investigated. The excited state behavior of **1a** within zeolites discussed in detail below helps to establish the various factors that need to be controlled during the chiral photoreduction process.

Phenyl cyclohexyl ketone (**1a**)[20,21] in isotropic solution gives a γ-hydrogen abstraction Norrish–Yang cleavage product (**2a**; Scheme 5). As expected based on solution behavior, irradiation as a hexane slurry of **1a** included within NaY gave **2a** as the only product. On the other hand, irradiation of **1a** included within optically pure ephedrine, pseudoephedrine or norephedrine modified NaY gave intermolecular hydrogen abstraction product **3a**, in addition to **2a**. The alcohol **3a** was the product of electron transfer from the amino group of the above chiral inductors to

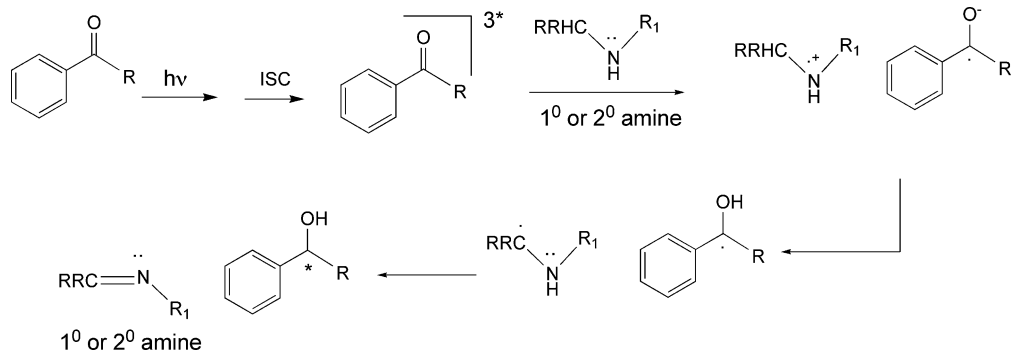

Scheme 4 Mechanism of electron transfer mediated photoreduction.

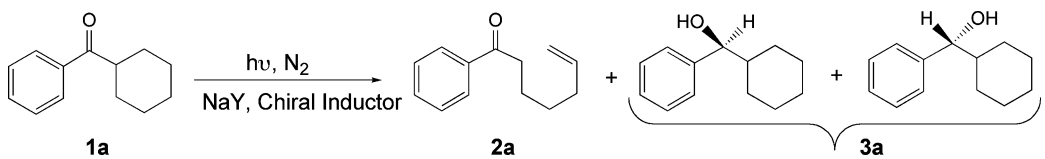

Scheme 5 Inter and intramolecular photoreduction of cyclohexyl phenyl ketone.

the excited ketone. Absence of formation of **3a** when ephedrine hydrochloride and (−)-diethyltartarate (no amino group) were used as chiral inductors confirms the need for a good electron donor to initiate the hydrogen abstraction process.

If the role of the amine was to serve as the electron donor, the ratio of inter *vs.* intramolecular hydrogen abstraction products (**2a** to **3a**) should depend on the electron donating ability of the chiral inductor. The ratio of **2a** : **3a** is expected to be lower when secondary amine chiral inductors such as ephedrine and pseudoephedrine are the donors than when the chiral inductor is a primary amine such as norephedrine. As predicted, for the same loading level of the chiral amine (one molecule per supercage) the ratio of **2a** : **3a** with norephedrine was 5 while that with pseudoephedrine was 0.20.

As indicated above, ketone **1a** included within a chirally modified (bearing amino group) NaY zeolite undergoes two primary photoreactions, one dependent and the other independent of the chiral inductor. For example, **1a** present in cages of types III and IV (Scheme 1) would give only **2a** whereas those present in cages of type V are expected to yield both **2a** and **3a**. This generalization predicts that the **2a** : **3a** ratio would depend on the ratio of the cages that contain the chiral inductor and those that do not, which in turn depends on the loading level of the chiral inductor. This expectation was also realized. Upon irradiation of **1a** included within NaY containing pseudoephedrine the ratio of **2a** : **3a** varied; at a loading level of one chiral amine per five supercages the ratio was 1.27 whereas at a loading level of one chiral amine per supercage the ratio was 0.20. Clearly, the amount of intermolecular reduction product increased with the increased loading level of pseudoephedrine. An additional important point to note is that although the ratio of **2a** to **3a** was dependent on the loading level of the chiral inductor, the ee was independent of the loading level of the chiral inductor. This observation supported the view that reduction occurred only in cages containing the chiral inductor. Had there been intermolecular reduction (to yield racemic products) in cages that do not contain the chiral inductor the ee would have increased with increased loading levels of the chiral inductor

While the ee obtained in this study is the highest amongst the thus far reported examples of photoreduction of achiral ketones,[19] unfortunately we are unable to develop a model that could be used to predict the extent of chiral induction within a zeolite. Several observations suggest that one must include the alkali ion in any mechanistic understanding of the asymmetric induction process within zeolites. The following experimental observations relating to the measured ee in the case of **1a** should be noted in this context: (a) the ee depends on the water content within NaY. Dry zeolites give higher ee than wet ones, (b) the ee depends on the number of alkali ions, (c) most importantly, the % ee depends on the nature of the alkali ion. Thus it is clear that to obtain maximum ee one should use a dry zeolite with moderate number of alkali ions (preferably Y zeolite). At this stage we are unable to predict which alkali ion would work best. Alkali ions play two roles in the chiral induction process. They forge a closer interaction between the ketone and the chiral amine. In addition they modulate the electron donating ability of the amine. Smaller ions such as Li^+ force a closer interaction but they drastically reduce the ability of the amine to donate electrons. Further larger ions such as Rb^+ and Cs^+ may not allow both the ketone and the amine to occupy the same cage. In addition one should keep in mind that the ability to dry zeolites with various alkali ions might differ. It is especially important to note that LiY is harder to dry than other zeolites. In general we have found that, to achieve chiral induction, Na^+ and K^+ ions are better than Rb^+ and Cs^+ ions.

One disappointing observation is that despite the entire reaction occurring within chirally modified cages, the ee is not quantitative. This, we believe, is due to the multi-step nature of the reaction involving at least three distinct intermediates, the triplet ketone, the radical ions and the radicals (Scheme 4). All three intermediates possess pro-chiral faces and the factors that control the addition to the pro-chiral faces of these intermediates are likely to be different. Both computational and solid state NMR results relate only to the ground state ketone and at this stage we do not have any experimental results that provide an understanding of the nature of interaction between the three reactive intermediates and the chiral amines. In spite of this deficiency we have been able to make some generalizations that are presented below.

We believed that to make generalizations it is important to assign the absolute configuration of the two alcohols formed during the photoreduction of cyclohexyl phenyl ketone and identify the peaks A and B in the GC/HPLC traces. This was achieved by synthesizing the optically enhanced α-cyclohexyl benzyl alcohol by a known procedure.[12] When ketone **1a** was reduced thermally by a known literature procedure using chiral inductor (*S*)-diphenyl pyrrolidine methanol, enantiomerically enriched α-cyclohexyl benzyl alcohol was obtained. About 65% enrichment of the *R* enantiomer was obtained in the product mixture which corresponded to the A isomer on the chiral GC trace. The authenticity of the configuration of the enantiomer was confirmed with the literature report. In Table 2 the enantiomer that is enhanced by each chiral amine is indicated.

On examination of the results of chiral induction with various chiral amines a few generalizations result. The ephedrine family of inductors comprising norephedrine, ephedrine, pseudoephedrine, *N*-methylephedrine, aminophenylethanol, aminophenylpropanediol and aminomethoxyphenylpropanol provided an interesting comparison. It was observed that chiral inductors with the *S* configuration at the benzylic alcohol part always favored the *R* enantiomer of α-cyclohexyl benzyl alcohol. This point becomes clear when one notices that the inductor (*S*)-aminophenylethanol that does not have any chiral carbon connected to the amino group gave an ee of 26% *R*. We tentatively conclude that the configuration at the benzylic alcohol portion of the chiral inductor determines the absolute configuration of the alcohol product.

Perusal of Table 2 reveals that the probability of getting chiral induction from chiral inductors possessing two or more functional groups like amino and hydroxyl was greater than for those with monofunctional groups. For example, norephedrine (68% ee) and pseudoephedrine (37% ee) gave higher ee's compared to α-methylbenzylamine (8% ee). It was also seen that the phenyl group was important in the chiral induction process. Norephedrine and other ephedrine family inductors that possess hydroxyl, phenyl and amino groups were very successful compared to the ones lacking a phenyl group such as valinol and alaninol. The nature of the amine also seems to matter: Comparing norephedrine, ephedrine and *N*-methyl ephedrine (Scheme 3), it can be seen that all three inductors have similar structural features and chiral configurations (1*S*,2*R*), except that norephedrine is a primary

amine, ephedrine is a secondary amine and *N*-methyl ephedrine is a tertiary amine. The ee's obtained from these vary from 68% to 16% to 27%, all enhancing the *R*(+) enantiomer in the α-cyclohexyl benzyl alcohol. Thus there is a complex relationship between the chiral inductor and the extent of chiral induction. With the results on hand it is too difficult to present a model for electron transfer mediated photoreduction within zeolites. We have established that with the help of zeolites one can obtain significant chiral induction in the electron transfer mediated photoreduction of carbonyl compounds. The mechanistic details are yet to be established.

Conclusions

We have shown with several examples that electron transfer mediated photoreduction of carbonyl compounds could be achieved within zeolites. More importantly, the product obtained when a chiral amine is used is enantiomerically enriched. The role of zeolite is obvious when one recognizes that the product alcohol is formed as a racemic mixture in solution. The best enantiomeric excess obtained within a zeolite is 68%. This chiral induction is far higher than that reported in solution during the electron transfer mediated photopinacolization of acetophenone at room temperature. The role of cations in forcing a closer interaction between a reactant and a chiral amine is revealed by solid state NMR and computational results. At this stage we are unable to present a model that would predict the absolute configuration of the optical isomer that would be enhanced. Further experiments are needed to achieve this goal.

Experimental

(a) Materials

Sigma-Aldrich samples of phenyl cyclohexyl ketone (**1a**), phenyl isopropyl ketone (**1b**), phenyl cyclopentyl ketone (**1c**), 4′-methoxyacetophenone (**1e**), 2-methylbenzophenone (**1k**), 4-methylbenzophenone (**1l**), 2-chlorobenzophenone (**1m**), 4-chlorobenzophenone (**1n**) and 2-methoxyacetophenone (**1o**), and 2-methoxybenzophenone (**1h**) from Lancaster synthesis were used as received. Ketones **1d**, **1f** and **1g** were synthesized following the procedure reported in the literature.[22] Ketone **1i** was synthesized by refluxing sodium methoxide (1 eq.) and the corresponding hydroxybenzophenone (1 eq.) and dimethyl sulfate (excess) in methanol for 12 h. Methanol was removed under reduced pressure, and the reaction mixture was dissolved in ether and washed several times with water. Products were isolated from the reaction mixtures by silica gel column chromatography using 10% ethyl acetate and hexane mixture as eluent. Ketone **1j** was prepared by refluxing 2-hydroxybenzophenone (1 eq.), potassium carbonate (1 eq.), dibenzo-18-crown-6 (0.5 eq.) and ethyl iodide (2 eq.) in acetonitrile for 12 h. Product was isolated by silica gel column chromatography using 10% ethyl acetate and hexane mixture as eluent. The procedure for the synthesis of ketones **1p** and **1q** was kindly provided by J. R. Scheffer and C. Scott. The chiral inductors used in this study were obtained from Aldrich and Fluka and used as received.

Commercial samples (Aldrich) of acetophenones for solid state NMR studies were distilled twice prior to use. Perdeuterated acetophenone was obtained from Cambridge Isotope Laboratories, Inc.

Zeolite NaY (Si/Al 2.4) was obtained from PQ Corporation. Zeolites LiY, KY, and RbY and CsY were prepared from the NaY zeolite sample by cation exchange using appropriate nitrate solution and refluxing at 90 °C for at least 3 h. A 10 mL aliquot of a 10% nitrate solution was used for each gram of zeolite, and the cation exchange was repeated three times. The exchanged samples were then thoroughly washed with water to remove sulfate and chloride ions. Exchange loading was typically between 60 and 84%.

Characterization of reactant ketones. Reactants **1a**, **1b**, **1c**, **1e**, **1h**, **1k**, **1l**, **1m**, **1n** and **1o** are commercially available from Sigma-Aldrich and Lancaster synthesis.

*Reactant **1d**.* ^{1}H NMR (400 MHz, $CDCl_3$) δ: 7.54–7.51 (m, 2H), 7.42–7.36 (m, 3H), 2.06–1.99 (m, 9H), 1.73–1.72 (m, 6H).

GC-MS (EI): 240 (M^+ 88), 135 (41), 105 (100), 77 (67).

*Reactant **1f**.* ^{1}H NMR (400 MHz, $CDCl_3$) δ: 1.12–2.22 (10H, m), 2.92–3.24 (1H, m), 3.82 (3H, s), 6.82 (2H, d, $J = 9$ Hz), 7.84 (2H, d, $J = 9$ Hz).

GC-MS (EI): 218 (M^+ 5), 135 (100), 107 (8), 92 (11), 77 (14).

*Reactant **1g**.* GC-MS (EI): 256 (M^+ 16), 201 (18), 187 (40), 173 (100), 145 (48), 83 (38).

*Reactant **1i**.* ^{1}H NMR (400 MHz, $CDCl_3$) δ: 7.8–7.6 (m, 4H), 7.5–7.3 (m, 3H), 6.9–6.8 (2H, m), 3.8 (3H, s).

*Reactant **1j**.* ^{1}H NMR (400 MHz, $CDCI_3$) δ: 1.01 (t, $J = 8$ Hz, 3H), 3.93 (q, $J = 8$ Hz, 2H), 6.94 (br d, $J = 8.4$ Hz, 1H), 7.02 (m, $J = 7.1$, 0.9 Hz, 1H), 7.36–7.46 (m, 4H), 7.52 (m, $J = 7.4$, 1.2 Hz, 1H), 7.78 (dd, $J = 8.4$, 1.1 Hz, 2H).

*Reactant **1p**.* ^{1}H NMR (400 MHz, $CDCl_3$) δ: 1.14–1.19 (m, 2H), 2.0–2.06 (m, 2H), 3.45 (t, 1H, $J = 1.3$ Hz), 3.64–3.65 (dd, 2H, $J = 3.6$ Hz), 7.12 (m, 2H), 7.19 (m, 2H), 7.45 (m, 2H), 7.55 (m, 1H), 7.95 (m, 2H)

GC-MS (EI): 248 (M^+, 30), 247 (3), 229 (3), 143 (21), 133 (17), 128 (92), 115 (21), 105 (100), 89(2), 77 (35).

*Reactant **1q**.* ^{1}H NMR (400 MHz, $CDCl_3$) δ: 1.14–1.19 (m, 2H), 2.0–2.06 (m, 2H), 3.45 (t, 1H, $J = 1.3$ Hz), 3.64–3.65 (dd, 2H, $J = 3.6$ Hz), 7.1–7.22 (m, 6H), 7.96–8.0 (m, 2H).

GC-MS (EI): 266 (M^+, 7), 247 (1), 151 (19), 143 (20), 129 (12), 128 (88), 123 (100), 115 (22), 95 (35), 89(3), 75 (5).

(b) Activation of zeolites

About 300 mg of the zeolite was placed in a silica crucible and heated at 500 °C for 12 h. The freshly activated zeolite samples were rapidly cooled in air to *ca.* 50 °C and then transferred into glass sample tubes, connected to a vacuum manifold, and degassed at 80 °C under low pressure (10^{-3} Torr). We observed that such a procedure facilitates the complete removal of water and other adsorbents.

(c) Characterization of photoproducts

Photoproducts were identified to be the corresponding alcohols from **1a–1q**. Their authenticity was confirmed by comparing with synthetic samples prepared from **1a–1q** through $NaBH_4$ reduction. Spectral data are provided below.

Alcohol from 1a. ^{1}H NMR (400 MHz, $CDCl_3$) δ: 0.85–1.42 (m, 6 H), 1.54–1.81 (m, 4 H), 1.89 (s, 1H), 1.92–2.03 (m, 1 H), 4.35 (d, 1 H, $J = 7.2$ Hz), 7.22–7.36 (m, 5 H).

GC-MS(EI): 190 (M^+, 7), 107(100), 79(34).

Alcohol from 1b. ^{1}H NMR (400 MHz, $CDCl_3$) δ: 0.79 (d, 3H), 1.02 (d, 3H), 1.92–1.99 (m, 2H), 4.35 (d, 1H), 7.25–7.37 (m, 5H).

GC-MS (EI): 150 (M^+, 13), 107 (100), 79 (50).

Alcohol from 1c. ^{1}H NMR (400 MHz, $CDCl_3$) δ: 7.35–7.22 (m, 5H), 4.39 (d, 1H), 2.24 (m, 1H), 1.92–1.15 (m, 8H).

GC-MS (EI): 176 (M^+, 8), 158 (52), 129 (32), 115 (36), 107 (100), 91 (40), 79 (56), 67 (64).

Alcohol from 1d. ^{1}H NMR (400 MHz, $CDCl_3$) δ: 7.25–7.33 (m, 5H), 4.2 (d, 1H), 1.96 (m, 3H), 1.84 (d, 1H), 1.47–1.72 (m, 12H).

GC-MS (EI): 242 (M^+, 4), 135 (100), 107 (13), 93 (18), 79 (30).

Alcohol from 1e. ^{1}H NMR (400 MHz, $CDCl_3$) δ: 1.44 (d, $J =$ 6.3 Hz, 3H), 2.76 (br, 1H), 3.77 (s, 3H), 4.78 (q, $J = 6.3$ Hz, 1H), 6.83–6.91 (d, $J = 8.3$ Hz, 2H), 7.22–7.31 (d, $J = 8.3$ Hz, 2H).

GC-MS (EI): 152 (M^+, 31), 137 (100), 109 (65), 94 (38), 77 (43).

Alcohol from 1f. ^{1}H NMR (400 MHz, $CDCl_3$) 7.18 (d, $J =$ 8.4 Hz, 2H), 6.84 (d, $J = 8.4$ Hz, 2H), 4.25 (d, $J = 7.6$ Hz, 1H), 3.77 (s, 3H), 1.99–1.97 (m, 2H), 1.75–1.72 (m, 1H), 1.63-1.54 (m, 3H), 1.34–1.31 (m, 1H), 1.29–0.83 (m, 5H).

GC-MS (EI): 220 (M^+, 3), 202 (8), 137 (100), 121 (10), 109 (20), 94 (13), 77 (10).

Alcohol from 1g. GC-MS (EI): 258 (M^+, 4), 175 (100), 147 (8), 127 (30), 83 (92).

Alcohol from 1h. ^{1}H NMR (400 MHz, $CDCl_3$) δ: 3.12 (s, br, 1H), 3.80 (s, 3H), 6.05 (s, 1H), 6.89 (d, 1H, $J = 8.3$ Hz), 6.92–6.96 (m, 1H), 7.20–7.33 (m, 5H), 7.37–7.41 (m, 2H).

Alcohol from 1i. ^{1}H NMR (400 MHz, $CDCl_3$) δ: 2.19 (s, br, 1H), 3.78 (s, 3H), 5.80 (s, 1H), 6.84–6.89 (m, 2H), 7.24–7.39 (m, 7H).

Alcohol from 1k. ^{1}H NMR (400 MHz, $CDCl_3$) δ: 2.26 (s, 3H, CH_3), 2.38 (s, 1H), 6.00 (s, 1H), 7.15–7.36 (m, 8H), 7.53 (d, $J =$ 8.0 Hz, 1H).

Alcohol from 1l. ^{1}H NMR (400 MHz, $CDCl_3$) δ: 2.00 (s, br, 1H), 2.32 (s, 3H), 5.76 (s, 1H), 7.05–7.38 (m, 9H).

Alcohol from 1m. ^{1}H NMR (400 MHz, $CDCl_3$) δ: 2.46 (s, 1H), 6.11 (s, 1H), 7.11–7.30 (m, 8H), 7.51 (d, $J = 7.5$ Hz, 1H).

Alcohol from 1n. ^{1}H NMR (400 MHz, $CDCl_3$) δ: 2.21 (s, br, 1H), 5.76 (s, 1H), 7.20–7.45 (m, 9H).

Alcohol from 1o. ^{1}H NMR (400 MHz, $CDCl_3$) δ: 1.50 (d, 3H, $J = 6.6$ Hz), 2.72 (s, 1H), 3.86 (s, 3H), 5.08 (m, 1H), 6.86–7.36 (m, 4H).

Alcohol from 1p. ^{1}H NMR (400 MHz, $CDCl_3$) δ: 1.14–1.19 (m, 2H), 2.0–2.06 (m, 2H), 2.17–2.22 (m, 1H), 2.7 (m, 1H), 3.6 (m, 1H), 4.5 (d, 1H), 6.8–7.1 (m, 4H), 7.19 (m, 2H), 7.3–7.42 (m, 3H).

GC-MS (EI): 250 (M^+, 30), 230 (4), 219 (10), 204 (16), 190 (13), 176 (6), 148 (18), 143 (100), 133 (47), 130 (87), 129 (24), 128 (77), 116 (35), 115 (60), 107 (34), 105 (27), 91(10), 77 (37), 58(27).

Alcohol from 1q. ^{1}H NMR (400 MHz, $CDCl_3$) δ: 1.14–1.18 (m, 2H), 1.98–2.03 (m, 2H), 2.17–2.2 (m, 1H), 2.7 (m, 1H), 3.6 (m, 1H), 4.5 (d, 1H), 6.8–7.1 (m, 4H), 7.19 (m, 2H), 7.33–7.38 (m, 2H).

GC-MS (EI): 268 (M^+, 23) 250 (2), 229 (5), 219 (5), 151 (13), 144 (16), 143 (100), 130 (62), 129 (24), 128 (48), 116 (22), 115 (50), 97 (19), 77 (16).

(d) Analysis of the enantiomeric excess of optically active alcohol products

Enantiomers were resolved either with a HP 5890 series II gas chromatograph with Supelco β-dex 350/OV-1701, β-dex 120 capillary chiral columns or in Rainin HPLC with chiralcel OD, chiralpak AD and chiralpak AD-RH chiral columns depending upon the benzylic alcohol products. Enantiomeric excesses (%ee) were calculated using the formula [(area of A − area of B)/(area of A + area of B)] × 100.

(e) Asymmetric reduction of phenyl cyclohexyl ketone (1a)

Freshly distilled trimethylsilyl chloride (130 mg, 1.2 mmol) was added to a suspension of $NaBH_4$ (45 mg, 1.2 mmol) in dry THF (5 mL). After the mixture was heated at 70 °C for 1 h and allowed to cool to room temperature, a solution of (S)-α,α-diphenylpyrrolidinemethanol (25 mg, 0.1 mmol) in THF (2 mL) was added. When there was no gas emitted, a solution of phenyl cyclohexyl ketone (188 mg, 1 mmol) in THF (2 mL) was added very slowly with a gas-tight syringe. After the addition was complete, the mixture was hydrolyzed with 2 M HCl (5 mL) and extracted with ether (3 × 10 mL). The combined organic layers were washed with brine, and dried with sodium sulfate. Filtration followed by evaporation of solvent yielded the alcohols 65% enriched in the *R* isomer as determined by analysis on GC with Supelco β-dex 350/OV-1701 chiral column. The configurations of the alcohols were confirmed by comparing and verifying them with various literature reports on α-cyclohexyl benzyl alcohol.[12]

(f) Sample preparation for solid-state NMR

The preparation of samples for solid state NMR experiments consisted of two steps. The first one involved the loading of chiral inductors within the zeolite. About 300 mg of the activated zeolite was added to a solution (9.0 mL hexane and 1 mL chloroform) of about 20–25 mg of chiral inductor (ephedrine, pseudoephedrine or norephedrine) and was stirred for 12 hours. The loading of chiral inductor within zeolite was one molecule per supercage. The solution was then filtered using a sintered crucible. The zeolite/chiral inductor complex was then degassed on a vacuum line at 60 °C, typically for 12 hours under low pressure (10^{-3} Torr). To the degassed zeolite/chiral inductor complex, about 4 mg of acetophenone sample (acetophenone or perdeuterated acetophenone) (equivalent to one molecule per four supercages of MY zeolite) was added in a glovebag under a nitrogen atmosphere. The sample was then transferred to a vacuum manifold and degassed at 60 °C for typically 12 h under low pressure (10^{-3} Torr). Such a heating of the sample ensured the uniform adsorption of acetophenone or perdeuterated acetophenone. The degassed sample was then packed into a zirconia rotor with an O ring in a glove bag under nitrogen atmosphere. ^{1}H NMR studies of these

solid samples revealed that there was no adsorption of atmospheric moisture during the course of sample preparation.

(g) Solid-state NMR spectra

Solid-state ^{13}C NMR spectra were recorded at room temperature with a Bruker AVANCE DSX 300 spectrometer at a ^{13}C resonance frequency of 75.47 MHz. Each acquisition typically consisted of 12000 to 16000 free induction decay scans. The ^{1}H–^{13}C cross-polarization spectra (^{13}C CP-MAS) were obtained with a recycle delay of 2 s using a 90° pulse width of 6.5 μs and a contact time of 1.5 ms. All CP-MAS experiments were processed with line broadening at 100 Hz. The spectra were referenced at room temperature relative to TMS. All NMR figures were plotted using Bruker XWINPlot software.

(h) Computational details

All the computations were done using the Gaussian 98 suite of programs with the RB3LYP method and 6-31G(d) basis set. For all the computed structures, frequencies were calculated and were found to be positive.

Acknowledgements

V. R. thanks the NSF for financial support (CHE-0212042).

References

1 Y. Inoue, *Chiral Photochemistry*, ed. Y. Inoue and V. Ramamurthy, Marcell Dekker, New York, 2004.
2 Y. Inoue, *Chem. Rev.*, 1992, **92**, 741.
3 H. Rau, *Chem. Rev.*, 1983, **83**, 535.
4 B. Grosch and T. Bach, *Chiral Photochemistry*, ed. Y. Inoue and V. Ramamurthy, Marcell Dekker, New York, 2004.
5 Y. Inoue, H. Ikeda, M. Kaneda, T. Sumimura, S. R. L. Everitt and T. Wada, *J. Am. Chem. Soc.*, 2000, **122**, 406.
6 J.-P. Pete and N. Hoffmann, *Chiral Photochemistry*, ed. Y. Inoue and V. Ramamurthy, Marcell Dekker, New York, 2004.
7 J. R. Scheffer, *Chiral Photochemistry*, ed. Y. Inoue and V. Ramamurthy, Marcell Dekker, New York, 2004.
8 K. Tanaka and F. Toda, in *Organic Photoreactions in the Solid State*, ed. F. Toda, Kluwer, New York, 2002.
9 J. Sivaguru, A. Natarajan, L. S. Kaanumalle, J. Shailaja, S. Uppili, A. Joy and V. Ramamurthy, *Acc. Chem. Res.*, 2003, **36**, 509.
10 V. Ramamurthy, A. Natarajan, L. S. Kaanumalle, S. Karthikeyan, J. Sivaguru, J. Shailaja and A. Joy, *Chiral Photochemistry*, ed. Y. Inoue and V. Ramamurthy, Marcell Dekker, New York, 2004.
11 S. G. Cohen, A. Parola and G. H. Parsons, *Chem. Rev.*, 1973, **73**, 141.
12 B. Jiang, Y. Feng and J. Zheng, *Tetrahedron Lett.*, 2000, **41**, 10281.
13 J. Schaefer and E. O. Stejskal, *J. Am. Chem. Soc.*, 1976, **98**, 1031.
14 J. Schaefer and E. O. Stejskal, *Top. Carbon–13 NMR Spectrosc.*, 1979, **3**, 283.
15 E. O. Stejskal and J. D. Memory, *High-Resolution NMR in the Solid State*, Oxford University Press, New York, 1994.
16 D. Cizmeciyan, L. B. Sonnichsen and M. A. Garcia-Garibay, *J. Am. Chem. Soc.*, 1997, **119**, 184.
17 M. J. Frisch, G. W. Trucks, H. B. Schlegel, P. M. W. Gill, B. G. Johnson, M. A. Robb, J. R. Cheeseman, T. Keith, G. A. Petersson, J. A. Montgomery, K. Raghavachari, M. A. Al-Laham, V. G. Zakrzewski, J. V. Ortiz, J. B. Foresman, J. Cioslowski, B. B. Stefanov, A. Nanayakkara, M. Challacombe, C. Y. Peng, P. Y. Ayala, W. Chen, M. W. Wong, J. L. Andres, E. S. Replogle, R. Gomperts, R. L. Martin, D. J. Fox, J. S. Binkley, D. J. Defrees, J. Baker, J. P. Stewart, M. Head-Gordon, C. Gonzalez and J. A. Pople, in *Gaussian 98 Rev. A11*, Pittsburgh, PA, 1998.
18 P. Butz, R. T. Kroemer, N. A. Macleod, E. G. Robertson and J. P. Simons, *J. Phys. Chem. A*, 2001, **105**, 1050–1056.
19 D. Seebach, H. Dorr, B. Bastani and V. Ehrig, *Angew. Chem., Int. Ed. Engl.*, 1969, **8**, 982.
20 F. D. Lewis, R. W. Johnson and D. E. Johnnson, *J. Am. Chem. Soc.*, 1974, **96**, 6090.
21 J. H. Stocker and D. H. Kern, *J. Chem. Soc. D*, 1969, 204.
22 D. E. Bergbreiter and J. M. Killough, *J. Org. Chem.*, 1976, **41**, 2750.